IUBAT Review—A Multidisciplinary Academic Journal, 8(1): 96-112
https://doi.org/10.3329/iubatr.v8i1.83657

Development of a Low-cost Surface Wettability Measurement Instrument

Md. Mobashir Hosain[1], Debasish Sarker[2*]

[1]*Department of Mechanical Engineering, City University, Dhaka, Bangladesh, ORCID 0000-0002-3892-7923*

[2]*Department of Mechanical Engineering, International University of Business Agriculture and Technology, Dhaka, Bangladesh, ORCID 0000-0001-7888-2929*

Keywords:

Surface wettability; Contact angle measurement equipment; Static contact angle; Dynamic contact angle.

Abstract

This study presents the development and validation of a low-cost, computer-controlled device for measuring surface wettability through contact angle analysis. The instrument comprises electro-mechanical components operated by an Arduino Uno microcontroller, including a high-precision syringe pump, a 3-axis motorized workbench, and a mobile camera with a 100 mm macro lens. Surface preparation involved polishing, cleaning, and drying to ensure repeatable conditions. Water droplets (2–10 µL) were dispensed and withdrawn on aluminium, copper, brass, steel, and glass substrates under ambient laboratory conditions. Static and dynamic contact angles were extracted from 40 high-resolution images obtained from 30 fps video recordings and analysed using ImageJ and MATLAB. The device achieved static contact angle measurements of 93° ± 2.7° (Al), 85° ± 6.35° (Cu), 25.0° ± 6.7° (glass), 88° ± 8.35° (brass), and 87° ± 5° (steel), with deviations from literature values ranging from 1.93° to 4.97°. Dynamic analysis indicated higher contact angle hysteresis for copper and brass (~34°), while glass showed the lowest (~21°) at a flow rate of 0.8 µL/s. The instrument demonstrated high measurement precision, with uncertainties of ±3.5° for imaging and ±0.2° for angle calculation, validating it as an accurate and cost-effective alternative to commercial goniometers.

1. Introduction

A liquid layer spreads over a substrate, when a liquid droplet impinges on the substrate and it is referred as wetting. The interaction between the molecules of the solid and liquid characterizes wettability of a surface. The liquid contact angle quantifies the degree of wettability (Lamour *et al.* 2010). According to Young's equation, three interfacial forces act when the liquid droplet impinges on a surface.

*Corresponding author's E-mail address: dsarker.me@iubat.edu
Article received: October 2024 Revised and accepted: April 2025 Published: June 2025

The mechanical equilibrium of these forces is established by the liquid contact angle (ADAM 1957). This is mathematically demonstrated by Equation (1):

$$\gamma^{SV} - \gamma^{SL} = \gamma^{LV}\cos\theta \quad (1)$$

The surface tensions between the solid-vapor interface, the solid-liquid interface, the liquid-vapor interface are represented by γ^{SV}, γ^{SL}, and γ^{LV}, respectively. Figure 1 represents the illustration of contact angles on a smooth homogeneous solid surface. Surfaces are categorized as super hydrophilic ($0°<\theta<10°$), hydrophilic ($10° <\theta <90°$), hydrophobic ($90° <\theta <150°$), or super-hydrophobic ($150° <\theta <180°$) according to how effectively they absorb moisture.

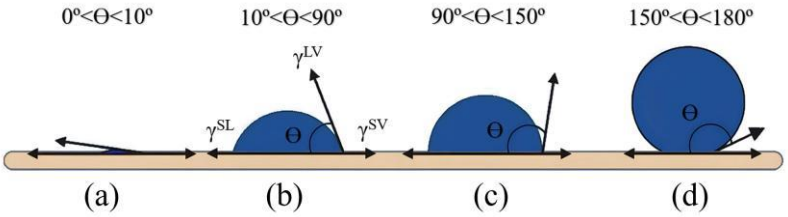

Figure 1. Illustration of contact angles on a smooth homogeneous solid surface.

A liquid spread over a solid surface when it is dispensed through a needle. An advancing liquid contact angle is created as a result of the substrate's pinning action on the liquid's wetting front. Upon redispersion of the liquid, a receding contact angle is observed. Surface-wetting qualities can be determined by utilizing the liquid contact angle hysteresis, which is the difference between the advancing (θadv) and receding (θrec) liquid contact angles on a surface (Gao & McCarthy, 2006). The contact angle hysteresis (θhys) is represented mathematically in equation (2).

$$\theta_{hys} = \theta_{adv} - \theta_{rec} \quad (2)$$

The substance becomes more hydrophobic as the strength of liquid-liquid interactions grows with the contact angle. Measuring surface wettability has garnered significant attention in the design of heat-exchanging surfaces, self-cleaning surfaces, biomedical equipment, oil/water separators, etc. (Samanta *et al.* 2020; Kong *et al.* 2018; Sun *et al.* 2021). Surface wettability has applications in energy conversion, oil–water separation, self-cleaning, emission control, bio-adhesion, and biomolecular immobilization (Jothi Prakash & Prasanth, 2021). Hydrophilic surfaces play a vital role in advancing applications in biomedicine, drug delivery, self-assembly systems, and everyday materials, as they enable a better understanding of water-attracting polymer behavior and design (Bayliss & Schmidt, 2023). It is essential for determining a solvent's capacity to dissolve and interact with polar compounds, which is particularly important for efficient extraction, separation, and analysis in aqueous environments (Zhang *et al.* 2023). On the other hand, hydrophobicity serves a different yet equally significant purpose. It enhances

the long-term durability of geopolymer concrete by reducing water ingress and thereby mitigating degradation in its inherently porous, hydrophilic structure (Sidhu & Kumar, 2023). Additionally, hydrophobicity is a key factor in the performance of anti-microbial peptides, as it governs their interaction with and disruption of bacterial membranes ultimately influencing both their antimicrobial efficacy and toxicity (Gagat *et al.,* 2024). Furthermore, hydrophobic properties improve the water resistance of wood, helping to prevent moisture absorption that can lead to swelling, cracking, decay, and reduced structural integrity over time (Jian *et al.*, 2023). So, the measurement of wettability is very important. However, due to the high cost of commercial goniometers, significant research has focused on developing low-cost alternatives. It is a prevalent trend to construct manual surface wettability testing equipment due to the high cost of surface wettability testing apparatus. To the best of the authors' knowledge, instruments for assessing surface wettability have recently been developed (Han, Shin & Ho Shin, 2022; Akbari & Antonini, 2021). The liquid contact angle can be optically measured using a simple apparatus (Lamour et al. 2010b). Manual and smartphone-based setups have proven suitable for static contact angle measurements but often lack the capability to accurately measure dynamic angles over time (Chen, Muros-Cobos & Amirfazli, 2018). For instance, a low-cost, 3D-printed contact angle measurement setup using smart devices offers an accessible educational tool, though its accuracy and precision are limited compared to laboratory-grade goniometers (Crowe *et al.*, 2021). A novel computer vision-based method enables accurate 3D reconstruction and contact angle measurement from nonorthogonal images using a smartphone setup, though it requires complex calibration and advanced image processing (Kumar & Chandraprakash, 2023). On absorbing substrates, contact angle measurements are further complicated by liquid uptake, requiring equal absorbed drop volumes to ensure consistency an added challenge under varying conditions (Krainer & Hirn, 2021). Other innovations include a low-cost goniometric system with motorized tilt and a circle-fit algorithm, which allows for accurate measurements on small sensors; however, its performance depends heavily on image quality and precise surface alignment (Sakti *et al.* 2017). In-house fabricated low-cost goniometers offer a functional alternative for measuring contact angle and surface tension, though they may lack the precision and durability of commercial systems (Sow & Y, 2020). A cost-effective, student-assembled setup for measuring both static and dynamic contact angles using the needle-in-drop method, enhancing practical understanding of surface wettability and interfacial phenomena across various scientific disciplines (Zou *et al.* 2024). Similarly, a smartphone-based goniometer constructed from locally available materials demonstrated accuracy rates exceeding 86% for organic samples and 94% for inorganic ones, validating its potential as an affordable substitute for commercial instruments (Chalise *et al.* 2023).

Given this background, our study aims to advance the field by developing a semi-automatic, computer-controlled contact angle measurement system capable of analyzing both static and dynamic contact angles with high accuracy and

repeatability. Unlike previous works, our approach combines motorized droplet control, automated imaging, and open-source software-based analysis, offering a balance of cost-efficiency, automation, and measurement precision. A comparative analysis of our methodology with existing approaches is presented in the Design Consideration section, highlighting the strengths and limitations of each to better situate our contribution in the evolving landscape of affordable wettability measurement technologies.

2. Components and Methods

2.1 Design Consideration

Despite recent advancements in low-cost and smartphone-based instruments for measuring surface wettability, several limitations persist. Existing setups are often constrained by their inability to accurately capture dynamic contact angles or require complex calibration procedures that limit accessibility and ease of use. While some studies have demonstrated promising accuracy levels, they typically rely on high-quality imaging conditions, precise surface alignment, or inconsistent calibration standards, particularly when applied to absorbing substrates. Moreover, many of these solutions are developed for educational or conceptual use and may not provide the robustness or reproducibility needed for rigorous scientific applications. To the best of the authors' knowledge, there remains a lack of a simple, cost-effective, and accurate system that can reliably measure both static and dynamic contact angles across varying substrate conditions. This research aims to address this gap by developing and validating a novel, accessible contact angle measurement system tailored for broader practical use. The standard measurement procedure for surface wettability is explained in the open literature. The measurement of contact angles involves several steps: surface preparation, placing a droplet of liquid onto a flat solid surface, ensuring standard droplet size and shape, controlling ambient conditions, conducting data analysis, and measuring the angle formed between the liquid-air interface and the solid-liquid interface at the three-phase contact line (Kwok & Neumann, 1999).

2.2 Surface preparation

The roughness of the surface affects contact angle measurements, which can be addressed by polishing and grinding (Islam, Tong & Falzon, 2014). For smooth surfaces, cleaning and drying are usually sufficient. However, for rough surfaces, additional techniques such as polishing or sandblasting may be necessary (Torrisi & Scolaro, 2015). Surface preparation is a critical stage in the measurement process as it directly impacts the accuracy of the contact angles. Cleaning the surface is essential, and solvent cleaning, plasma cleaning, and ultrasonic cleaning are commonly used techniques. Drying the surface after cleaning is crucial to remove any remaining solvent or moisture that could affect the measurement. Atmospheric air or nitrogen gas can be used for the drying process.

2.3 Droplet size and dispensing speed

The size of the water droplet influences the accuracy and precision of the measurement. Smaller droplets form more stable shapes, making the measurement of the liquid contact angle easier. However, evaporation can occur quickly with smaller drops, which may affect the contact angle measurement. Using drops that are too small can also result in a smaller contact area with the surface, affecting measurement accuracy. Therefore, excessively small drops can lead to erroneous results. A large droplet is affected by gravitational acceleration (Ryan & Poduska 2008), it is recommended to use droplets ranging between 5 and 10 µL. For dynamic measurements, the drop size should vary between 3 and 10 µL. To avoid dynamic effects, the minimum injection flow rate of the measurement device should be 0.05 µL/s, with a typical flow rate of 2 µL/s (Huhtamäki *et al*. 2018). Proper alignment of the camera with the surface of the liquid and the solid substrate is crucial. The substrate should be positioned on a flat base, and the camera lens should be aligned directly perpendicular to the surface of the substrate, with a slight downward tilt of 1°–3° to ensure a clear view (Huhtamäki *et al.* 2018).

2.4 Methods

2.4.1 Methodology

Electro-mechanical components are used in this device and they are operated by computer. The components are optimized and open-source numerical algorithm are used to develop the device at a very low cost. It is designed to achieve standard droplet volumes and accurately control dispensing and re-dispensing speeds. Vibration generated by the syringe pump is minimized. The 3-axis computer-controlled working table enables precise positioning and recording at different locations for repetitive measurements. A 100 mm distortion-free mobile camera compatible with a universal macro lens (APEXEL HD) has been used to capture high-quality, sharp images. Figure 2 illustrates the schematic diagram and a real image of our developed device.

The movement of the working bench in the test setup and the dispensing/suctioning of the liquid droplet system are facilitated by a high-reduction compound gear train with a rack and pinion mechanism. This setup utilizes a 5-volt 28BYJ-48 stepper motor with a ULN2003 motor driver. To ensure extra torque for movement along the Z-axis, two stepper motors with rack and pinion gear setups are connected in parallel. For movement along the X and Y-axis, a single stepper motor is used for each axis. The syringe pump is equipped with a compound gear train and rack and pinion mechanism to ensure accuracy and precision. It has a syringe diameter of 4 mm and a maximum dispensing/retracting speed of 3.44 µL/s. The deviation of droplet volume and dispensing/retracting speed is 0.1 µL and 0.01 µL/s, respectively. Figure 3 illustrates the syringe pump.

The syringe pump and the workbench of this device consume very low electrical power. They are controlled by the Arduino Uno, which is powered directly from the PC. The removable syringe arrangement provides flexibility when testing

with different liquids. A simple, user-friendly interface was achieved with the help of the Arduino IDE and a SCRCPY application. These applications are used to control the device and the smartphone camera from the computer. The screws at the base of the setup allow for adjustment of the working table's level.

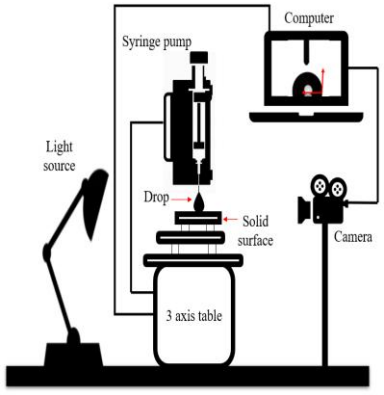

(a)

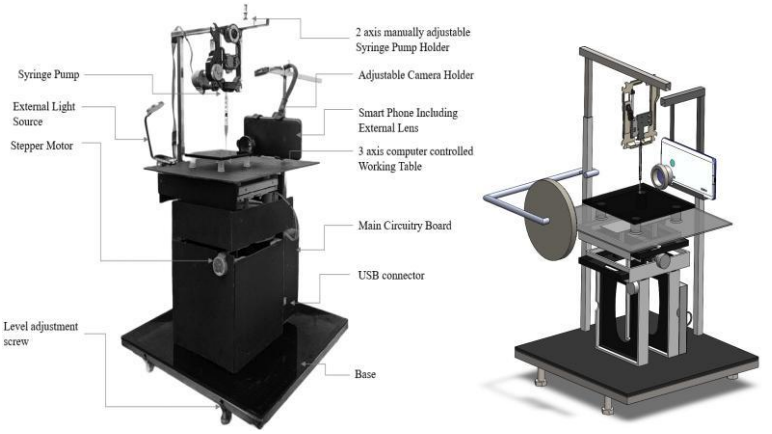

(b)

Figure 2. a) Schematic diagram, and b) a snapshot of the wettability testing apparatus and a CAD model.

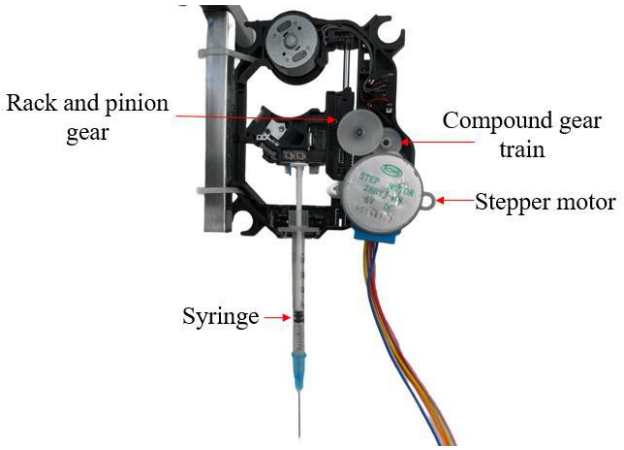

Figure 3. The syringe pump.

2.4.2 Imaging and Analyzing Techniques

The distortion-free, high-quality, 100 mm macro lens compatible with mobile phones reduces additional camera and lens costs. An external light source was also used to enhance image quality. For static liquid contact angle measurement (Huhtamäki *et al.* 2018), droplets (5-10 µL) were deposited at various locations on the surface. Dynamic measurement was initiated by depositing a 2 µL droplet on the test specimen. The droplet volume increased from 3 to 10 µL for measuring the advancing liquid contact angle.

Images were captured by the camera, and the data processing and analysis involved several software tools, including MATLAB, ImageJ, a free video-to-JPG converter, and Format Factory. The static liquid contact angle was analyzed using ImageJ. An open-source MATLAB code was also used to process the images and determine the liquid contact angle. Figure 4 illustrates the workflow of the code. This code was also utilized for measuring dynamic contact angles (Osborne, 2008). A series of images extracted from the video were processed. The code converts an image to grayscale values and subtracts the background noise to obtain homogeneity in pixel value distribution. It identifies the interfaces and fills up the holes in the droplets. Then the substrate surface is isolated and the best-fit circle is overlayed on the droplet. Out of this information, the contact angle has been determined. A user can copy the images to the code's working directory. The area of interest and the baseline of the droplet from two random images are set into the code. Subsequently, the code executes all queries sequentially, determining the contact angle of each image from the directory and displaying the output. An exemplary sequence of images for advancing liquid contact angle measurement is depicted in Figure 5a. When the droplet volume reached 10 µL, the syringe pump withdrew liquid from the surface, causing the liquid contact angle to decrease, as shown in Figure 5b. Figures 5a and 5b represent images for determining dynamic contact angles via the MATLAB code.

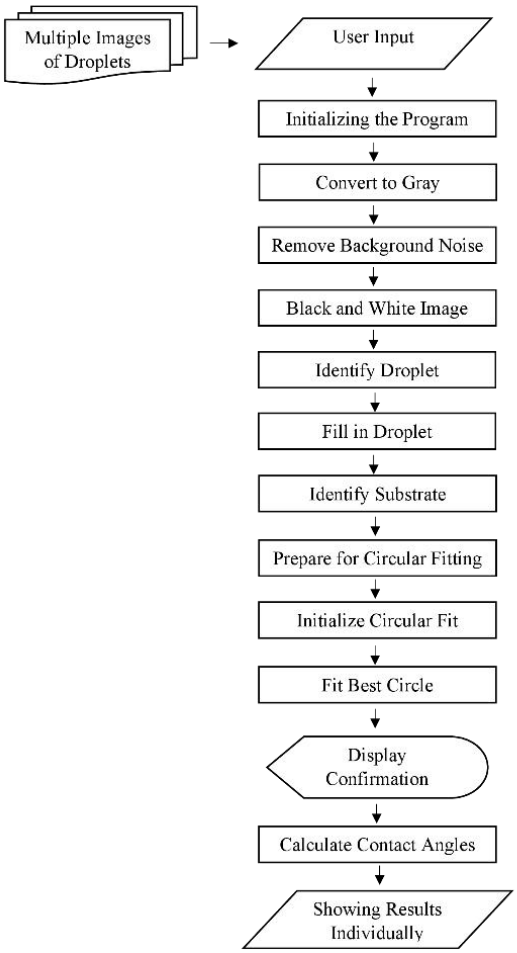

Figure 4. Flowchart for analyzing contact angle from series of images (adopted from Kosborne (Osborne 2008).

The recording resolution of our camera is 1920 x 1080 pixels, and the recording speed is 30 frames per second (fps). The video was analyzed frame by frame, with a pulse rate of every 0.5 seconds. A total of 40 images from the video were analyzed for each measurement. The uncertainty of imaging and measurement is ±3.5° and ±0.2°, respectively. The first frame of fig. 5a shows that a droplet of 2.4 µL is dispensed on a substrate at 0.5 s and it continues to grow up to 10 s. The contact angle between liquid and solid surface increases with the droplet size. On the other hand, the contact angle decreases as the needle sucks in water droplet from the surface (Figure 5b).

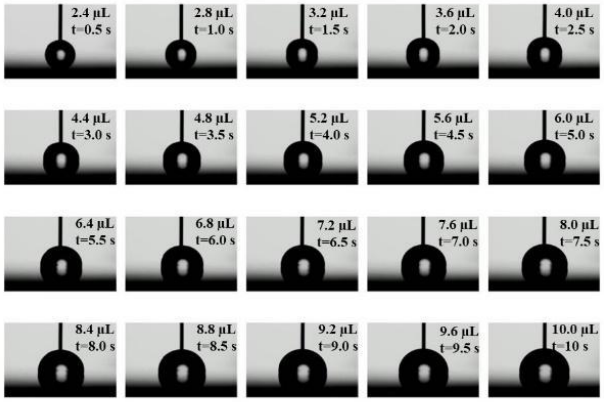

Figure 5a. Advancing contact angle with dispensing rate 0.8 µL/s.

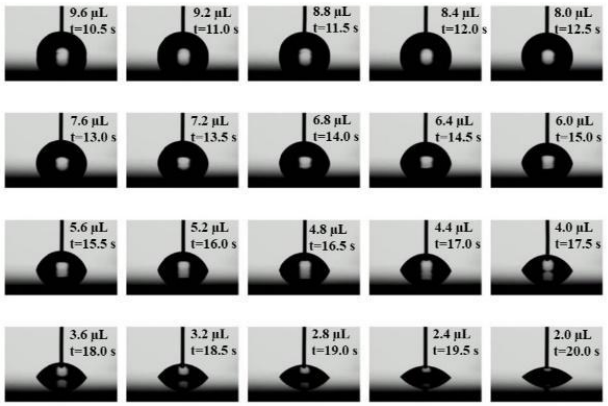

Figure 5b. Receding contact angle with re-dispensing rate 0.8 µL/s.

Table 1. Comparative Analysis of a Low-Cost DIY Contact Angle Measurement System Versus Commercial and Other Open-Source Alternatives.

Factor	**This Work (Your Setup)**	**Commercial Devices**	**Other Open-source Designs**
Cost	Very ow about $100 excluding mobile phone (DIY with open-source tools and mobile camera)	High (Typically $3,000–$12,000)	Low to Moderate (Approx. $200–$2000 depending on components)
Imaging Device	Smartphone with 100 mm distortion free macro lens	High-resolution industrial camera + zoom lenses	Varies: webcams, Smartphone or DSLRs commonly used
Resolution (Video)	1920×1080 pixel at 30 fps	Typically, > 2MP at 60–200 fps	Varies: HD to Full HD

Flowrate	4.8 µl/min to 206.4 µl/min	1 µl/min to 100 µl/min	Varies
Accuracy (Contact Angle)	±0.2° measurement accuracy; ±3.5° imaging uncertainty	Typically, ±0.1° or better	±1° to ±5° depending on implementation
Droplet Volume Control	Syringe pump, compound gear train with rack and pinion mechanism; ±0.1 µL volume accuracy	Motorized precision syringes (0.01 µL or better)	Stepper or servo-based systems; less consistent
Software Control	Semi- automated, Computer-controlled (Arduino IDE + SCRCPY + MATLAB + ImageJ)	Proprietary software (with real-time analytics and automation)	Open-source (Python, MATLAB, ImageJ)
Measurement Types	Static & dynamic (advancing and receding angles)	Static, dynamic, tilting, roll-off angle	Mostly static; some dynamic with limitations
Repeatability	Moderate (affected by vibration, alignment, surface pinning)	High (precision actuators and controlled environments)	Variable; often poor due to design constraints

This table 1 highlights key differences in cost, hardware components, resolution, fluid control, software integration, measurement capabilities, and repeatability among the presented DIY setup, commercially available contact angle measurement devices, and other open-source designs.

3. Results and Discussion

For the measurement of dynamic contact angles, de-ionized (DI) water was utilized as the test liquid due to its purity and consistent surface tension properties. The process began with initiating the 'run' command in the control software, which activated the syringe pump system. This command triggered the stepper motor to drive the syringe plunger downward, causing a controlled injection of DI water through a fine needle at a predetermined flow rate. As the water exited the needle, it gradually formed a droplet on the surface of the test substrate.

During the initial phase of droplet growth, the contact line between the liquid and solid surface expanded outward, resulting in the formation of an advancing contact angle. The expansion of the droplet was closely monitored in real-time. Once the droplet reached the desired volume and contact area, the stepper motor was halted by issuing a stop command through the software interface.

Subsequently, to initiate the receding contact angle measurement, a reverse command was given to the stepper motor, prompting it to rotate in the opposite direction. This reversed motion pulled the syringe plunger upward, thereby generating a negative pressure within the system. As a result, the DI water was gradually withdrawn from the droplet, causing it to shrink while maintaining contact with the substrate. This withdrawal led to the contraction of the contact line and facilitated the formation of the receding contact angle.

To ensure accurate and comprehensive analysis, the entire sequence was recorded at three distinct points during the injection and withdrawal process using a high-resolution video capturing system. These recordings enabled precise evaluation of the dynamic contact angles both advancing and receding providing valuable insights into the wettability characteristics of the substrate surface.

The substrates used in our measurements were Aluminum (Aluminum Alloy 6082), Copper, Steel (BS970 230M07-EN1A), Brass, and untreated Glass. Except for glass, all substrates were scrubbed with 600-grade emery paper for 3 minutes, and 800-grade emery paper for 1.5 minutes. Afterward, the substrates underwent thorough polishing for 1.5 minutes using 1000-grade emery paper, followed by a 1-minute abrasion with 2000-grade emery paper to attain a consistent surface topography. The specimens are depicted in Figure 6. Images of the specimens were captured using a Macro Lens capable of 100x magnification. The length scales of all the images are the same, and the topographies of the samples indicate that the Stainless surface is smoother than the others, while Copper sample exhibiting the roughest topology. Prior to the testing procedure, the substrates were wiped with cotton fabric soaked in 96% ethanol to remove impurities such as dust, oils etc. Additionally, the substrates were soaked in 96% ethanol for 15 minutes and dried in a dust-free atmosphere to ensure the contamination-free samples.

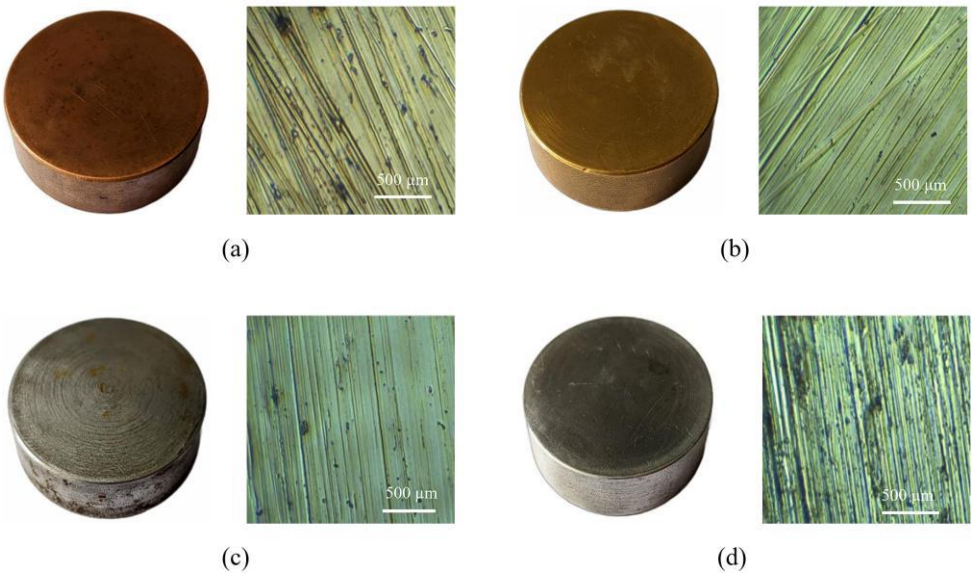

Figure 6. Specimen and surface topography (@100x magnification) for testing purpose (a) Copper, (b) Brass, (c) Steel, and (d) Aluminum.

Deionized water was used for liquid contact angle measurement. The 'run' command in the software allowed deionized water to be dispensed through the needle at a specified speed. As water was injected, the droplet size on the substrate increased, indicating the formation of the advancing contact angle. Once the water droplet reached the desired size, the stepper motor was given two commands: one

to stop and the other to reverse its spin. This action caused the plunger of the syringe pump to move upward, creating negative pressure that removed water from the substrate and formed a receding contact angle. The video was recorded at three different points to measure the liquid contact angles. Figure 7 (a) illustrates the advancing contact angle measurement, while Figure 7 (b) depicts the procedure for measuring the receding contact angle. The measurement results from the test setup are presented in Table 2.

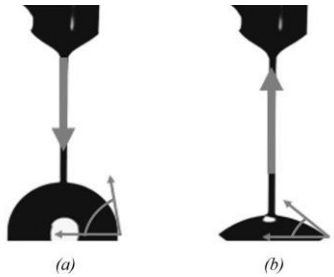

Figure 7: (a) Advancing and (b) receding contact angle.

Table 2. Surface wettability for different materials measured dynamically.

Test Specimen	Advancing, θ_{adv} (°)			Receding, θ_{rec} (°)			Hysteresis, θ_{hys} (°)		
	Point 1	Point 2	Point 3	Point 1	Point 2	Point 3	Point 1	Point 2	Point 3
Aluminum	95.85	95.90	94.70	70.20	70.95	67.40	25.65	24.95	27.30
Copper	89.30	91.80	86.65	66.45	61.50	51.85	22.85	30.30	34.80
Steel	90.60	90.40	91.55	60.30	60.55	62.70	30.30	29.85	28.85
Brass	89.30	89.15	87.55	60.45	56.60	53.75	28.85	32.55	33.80
Glass	26.80	25.00	36.65	18.60	13.35	15.61	08.20	11.65	21.04

The results of both static and dynamic measurements are depicted in Figures 8 (a-f), which include a bar chart and temporal evolution of contact angle graphs. Figure 8 (a) illustrates the static measurement of the liquid contact angle. The static contact angle measurements are as follows: 93.07º± 2.65º for aluminum, 85.35º±6º for copper, 25.69º±6º for glass, 88.34º±8º for brass, and 87.5º±4.5º for steel. The static contact angle measurement of aluminum was compared with different studies for validation purposes, where a dedicated measuring device was employed (Drelich, Miller & Hupka 1993; Kuznetsov, Feoktistov, Orlova, Batishcheva, & Ilenok, 2019; Kuznetsov, Feoktistov, Orlova, Zykov & Islamova, 2019). The maximum deviation was 4.97º and the minimum was 1.93º, with a percentage error range from 5.64% to 2.03%. Therefore, it can be inferred that these measurements are in good agreement with those obtained from a dedicated commercial device. Based on these results, it can be inferred that glass is hydrophilic, while aluminum

exhibits slight hydrophobicity. Other samples (copper, brass, steel) gave similar wettability.

Graphs 8 (b-f) depict the advancing and receding contact angle measurements. Points 1, 2, and 3 represent three measurements at different locations of each sample. The graphs suggest that the contact angle remains almost constant for up to 10 seconds. Water was dispensed on the substrates for this period of time. These angles indicate the advancing contact angle. Subsequently, the angle gradually decreases from 10 seconds to 20 seconds due to suction of water, reaching a plateau or the minimum contact angle values, representing the receding contact angle. To obtain the advancing contact angle of a sample, all advancing contact angles of that sample were averaged. Similarly, for the receding contact angle of a sample, all receding contact angles were averaged. However, the data sometimes fluctuates instead of gradually decreasing due to the vibration of the needle and the pinning effect of the surface during the dispensing or re-dispensing of the liquid droplets. Therefore, the graph may not appear completely smooth. The advancing contact angles were found to be 95.90º, 91.80º, 91.55º, 89.30º, and 36.65º for aluminum, copper, steel, brass, and untreated glass surfaces, respectively. Accordingly, the receding contact angles for the same materials were found to be 67.40º, 51.85º, 60.30º, 53.75º, and 13.35º. Hence, the maximum contact angle hysteresis values for these surfaces were determined to be 27.30º, 34.80º, 30.30º, 33.80º, and 21.04º.

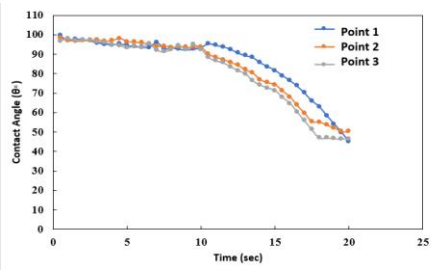

(b)

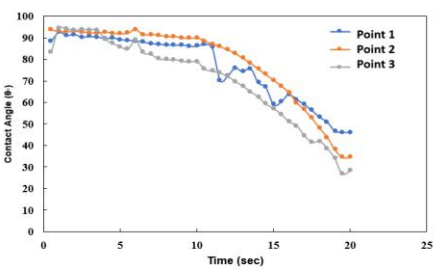

(c)

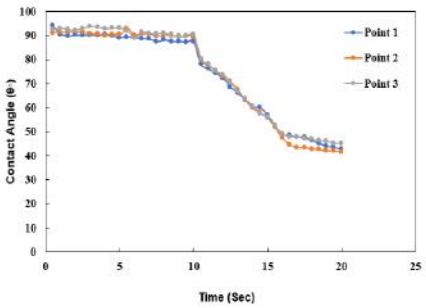

(d)

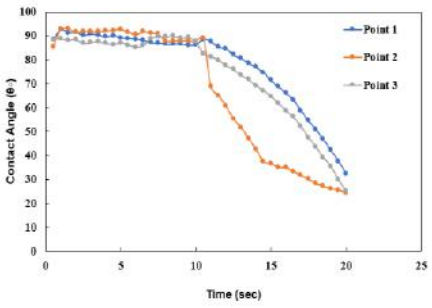

(e)

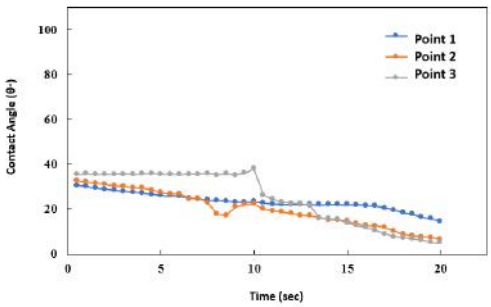

(f)

Figure 8: Represents the static and dynamic contact angle measurements (a) Static contact angle measurements for different materials with 10 µL droplets. (b) Temporal evolution of contact angle on an Aluminum substrate. (c) Temporal evolution of contact angle on a Copper substrate. (d) Temporal evolution of contact angle on a Steel substrate. (e) Temporal evolution of contact angle on a brass substrate. (f) Temporal evolution of contact angle on a glass substrate.

Errors during contact angle measurements are often inevitable due to the sensitivity of the setup to various internal and external factors. Mechanical vibrations from the syringe pump or stepper motor can disturb droplet stability, while surface roughness and contact line pinning led to inconsistent droplet shapes. Environmental conditions such as temperature and humidity can further affect droplet evaporation and spreading dynamics. Additionally, errors can arise from image processing limitations, inconsistent lighting, and manual frame selection, which introduces human bias. To minimize these issues, it is essential to improve mechanical isolation, ensure consistent substrate preparation, control environmental conditions, and adopt automated and high-resolution imaging systems to enhance measurement repeatability and accuracy.

5. Conclusion

Wettability is a very important parameter to characterize the surfaces. Designing of efficient heat exchangers, electronic cooling devices, surface coating etc. require the quantification of surface wettability property. The commercial surface wettability measurement tool is very expensive and ease-access to this technique is always not in the scope of every researcher. Therefore, a straightforward, effective, and affordable contact angle measurement tool has been fabricated in this study that worked well for measuring contact angles and accurately estimating the static and dynamic contact angles. A syringe pump, a 3-axis movable working bench, a high-resolution imaging technique, and an image processing technique are developed. An open-source MATLAB code was used for analyzing video data frame by frame. These techniques are combined together to determine the static and the dynamic

liquid contact angle. The standard measurement procedure was taken into consideration while designing the apparatus. Five substrates were prepared and their liquid contact angles were measured. The measured liquid contact angles are in good agreement with the available data in the open literature. Our devices are compatible with both academic and laboratory purposes because the range of error is low. A more user-friendly interface, and vibration free device could be in the scope of future development.

Conflict of interest

There is no conflict of interest according to authors best knowledge.

References

Adam, N. K. (1957). Use of the term 'Young's Equation' for contact angles. *Nature*, *180*(4590), 809-810.

Akbari, R., & Antonini, C. (2021). Contact angle measurements: From existing methods to an open-source tool. *Advances in Colloid and Interface Science*, *294*, 102470.

Bayliss, N., & Schmidt, B. V. (2023). Hydrophilic polymers: Current trends and visions for the future. *Progress in Polymer Science*, *147*, 101753.

Chalise, R., Niroula, A., Shrestha, P., Paudel, B., Subedi, D., & Khanal, R. (2023). A low-cost goniometer for contact angle measurements using drop image analysis: Development and validation. *AIP Advances*, *13*(8).

Chen, H., Muros-Cobos, J. L., & Amirfazli, A. (2018). Contact angle measurement with a smartphone. *Review of Scientific Instruments*, *89*(3).

Crowe, C. D., Hendrickson-Stives, A. K., Kuhn, S. L., Jackson, J. B., & Keating, C. D. (2021). Designing and 3D printing an improved method of measuring contact angle in the middle school classroom. *Journal of Chemical Education*, *98*(6), 1997-2004.

Drelich, J., Miller, J. D., & Hupka, J. (1993). The effect of drop size on contact angle over a wide range of drop volumes. *Journal of colloid and interface science*, *155*(2), 379-385.

Gagat, P., Ostrówka, M., Duda-Madej, A., & Mackiewicz, P. (2024). Enhancing antimicrobial peptide activity through modifications of charge, hydrophobicity, and structure. *International Journal of Molecular Sciences*, *25*(19), 10821.

Gao, L., & McCarthy, T. J. (2006). Contact angle hysteresis explained. *Langmuir*, *22*(14), 6234-6237.

Han, W., Shin, J., & Shin, J. H. (2022). Low-cost, open-source contact angle analyzer using a mobile phone, commercial tripods and 3D printed parts. *HardwareX*, *12*, e00327.

Huhtamäki, T., Tian, X., Korhonen, J. T., & Ras, R. H. (2018). Surface-wetting characterization using contact-angle measurements. *Nature protocols*, *13*(7), 1521-1538.

Islam, M. S., Tong, L., & Falzon, P. J. (2014). Influence of metal surface preparation on its surface profile, contact angle, surface energy and adhesion with glass fibre prepreg. *International Journal of Adhesion and Adhesives*, *51*, 32-41.

Jian, H., Liang, Y., Deng, C., Xu, J., Liu, Y., Shi, J., ... & Park, H. J. (2023). Research progress on the improvement of flame retardancy, hydrophobicity, and antibacterial properties of wood surfaces. *Polymers*, *15*(4), 951.

Jothi Prakash, C. G., & Prasanth, R. (2021). Approaches to design a surface with tunable wettability: a review on surface properties. *Journal of Materials Science*, *56*(1), 108-135.

Kong, X., Wei, J., Deng, Y., & Zhang, Y. (2018). A study on enhancement of boiling heat transfer by mixed-wettability surface. *Heat Transfer Engineering*, *39*(17-18), 1552-1561.

Krainer, S., & Hirn, U. (2021). Contact angle measurement on porous substrates: Effect of liquid absorption and drop size. *Colloids and Surfaces A: Physicochemical and Engineering Aspects*, *619*, 126503.

Kumar, A., & Chandraprakash, C. (2023). Computer vision-based on-site estimation of contact angle from 3-D reconstruction of droplets. *IEEE Transactions on Instrumentation and Measurement*, *72*, 1-8.

Kuznetsov, G. V., Feoktistov, D. V., Orlova, E. G., Batishcheva, K., & Ilenok, S. S. (2019). Unification of the textures formed on aluminum after laser treatment. *Applied Surface Science*, *469*, 974-982.

Kuznetsov, G. V., Feoktistov, D. V., Orlova, E. G., Zykov, I. Y., & Islamova, A. G. (2019). Droplet state and mechanism of contact line movement on laser-textured aluminum alloy surfaces. *Journal of colloid and interface science*, *553*, 557-566.

Kwok, D. Y., & Neumann, A. W. (1999). Contact angle measurement and contact angle interpretation. *Advances in colloid and interface science*, *81*(3), 167-249.

Lamour, G., Hamraoui, A., Buvailo, A., Xing, Y., Keuleyan, S., Prakash, V., & Borguet, E. (2010). Contact angle measurements using a simplified experimental setup. *Journal of chemical education*, *87*(12), 1403-1407.

Osborne, K. (2008). Determining the Contact Angle of a Droplet on a Substrate. *Major Qualifying Project, Worcester Polytechnic Institute, Worcester, MA*.

Ryan, Bernard J., and Kristin M. Poduska. 2008. "Roughness Effects on Contact Angle Measurements." American Journal of Physics 76 (11): 1074–77. https://doi.org/10.1119/1.2952446.

Sakti, S. P., Aji, R. Y., Amaliya, L., & Masruroh, M. (2017). Low-Cost Contact Angle Measurement System for QCM Sensor. *TELKOMNIKA (Telecommunication Computing Electronics and Control)*, *15*(2), 560-569.

Samanta, A., Wang, Q., Shaw, S. K., & Ding, H. (2020). Roles of chemistry modification for laser textured metal alloys to achieve extreme surface wetting behaviors. *Materials & design*, *192*, 108744.

Sidhu, J., & Kumar, P. (2023). Development of hydrophobicity in geopolymer composites-Progress and perspectives. *Construction and Building Materials*, *396*, 132344.

Sow, P. K., & Ashwin, Y. (2020). A design framework for the fabrication of a low-cost goniometer apparatus for contact angle and surface tension measurements. *Measurement Science and Technology*, *31*(12), 125401.

Sun, L., Guo, J., Chen, H., Zhang, D., Shang, L., Zhang, B., & Zhao, Y. (2021). Tailoring materials with specific wettability in biomedical engineering. *Advanced Science*, *8*(19), 2100126.

Torrisi, L., & Scolaro, C. (2015). Treatment techniques on aluminum to modify the surface wetting properties. *Acta Physica Polonica A*, *128*(1), 48-53.

Zhang, Y., Fu, R., Lu, Q., Ren, T., Guo, X., & Di, X. (2023). Switchable hydrophilicity solvent for extraction of pollutants in food and environmental samples: A review. *Microchemical Journal*, *189*, 108566.

Zou, Y., Ross, N., Nawaj, W., & Borguet, E. (2024). A Simplified Approach for Dynamic Contact Angle Measurements. *Journal of Chemical Education*, *101*(9), 3883-3890.